

ROYAL AIR FORCE
BEDFORD

R. & M. No. 3411



MINISTRY OF AVIATION

AERONAUTICAL RESEARCH COUNCIL
REPORTS AND MEMORANDA

Lift Due to Interference between an Aerofoil and an External Non-Lifting Body

BY S. NEUMARK, Techn.Sc.D., F.R.Ae.S.

LONDON: HER MAJESTY'S STATIONERY OFFICE

1965

PRICE 9s. 6d. NET

Lift Due to Interference between an Aerofoil and an External Non-Lifting Body

By S. NEUMARK, Techn.Sc.D., F.R.Ae.S.

COMMUNICATED BY THE DEPUTY CONTROLLER AIRCRAFT (RESEARCH AND DEVELOPMENT),
MINISTRY OF AVIATION

*Reports and Memoranda No. 3411**

May, 1964

Summary.

This paper contains an attempt to explain the incremental negative or positive lift induced on an aerofoil by an external non-lifting body (such as an engine nacelle), as observed in some experiments. A two-dimensional theory is proposed, based on representing the body by a system of sources and sinks, and by determining their effect on the aerofoil by means of a suitable conformal transformation. Two simple cases are considered: a semi-infinite body corresponding to a single source, and a finite body of oval shape corresponding to one source and one sink. Formulae for the induced-lift coefficient and for the position of centre of pressure are derived and illustrated by diagrams. Only incompressible flow is considered.

LIST OF CONTENTS

Section

1. Introduction
2. Case of Semi-Infinite Body
 - 2.1 Principles of the method
 - 2.2 Resultant forces and pitching moments from Blasius formulae
 - 2.3 Variation of induced lift with body position and size
 - 2.4 Variation of centre of pressure with body position
3. Case of a Finite Body of Oval Shape
 - 3.1 Theory and general discussion
 - 3.2 Numerical example
4. Concluding Remarks

Symbols

References

Appendices I and II

Illustrations—Figs. 1 to 8

Detachable Abstract Cards

* Replaces R.A.E. Tech. Note No. Aero. 2960—A.R.C. 26 188.

LIST OF APPENDICES

Appendix

- I. Semi-infinite body in two dimensions
- II. Finite body of oval shape in two dimensions

LIST OF ILLUSTRATIONS

Figure

1. Semi-infinite body obtained by combining uniform flow and single source
2. Aerofoil and semi-infinite body. Conformal transformation
3. Circulation induced by semi-infinite body. Loci of constant σ in physical plane
4. Circulation induced by semi-infinite body. Variation of σ along horizontals
5. Lift induced on aerofoil by semi-infinite body. Loci of source centres for constant C.P. positions
6. Finite body obtained by combining uniform flow, one source and one sink
7. Characteristic parameters of finite oval body
8. Aerofoil and finite body of oval shape

1. *Introduction.*

It has been found that, if an external non-lifting body (such as an engine nacelle) is situated near to a wing behind and above its trailing edge, there results an appreciable diminution of the wing lift. The phenomenon seems to admit an easy explanation in general terms: the flow of air above the wing being restrained by the obstacle, the velocities in this region are decreased, and the pressures increased, in comparison with those below the wing, and thus a negative incremental lift is produced. The analogous reasoning shows that a positive incremental lift should be induced by an external body located below the wing.

The numerical values of the decremental (or incremental) lift coefficient will not be very large in practical cases, but may easily reach 0.2 or even more. It might be argued that such an effect would not be very significant: a small increase of incidence would make up for the loss of C_L , so that the net effect would be only a slight increase in drag. However, the matter may assume considerable importance in some cases, and especially if an aircraft is designed to cruise at a combination of incidence and high subsonic Mach number, just below the conditions of compressibility drag rise. The external engine nacelles, located above and behind the inner part of the wing, may then cause a marked decrease of lift of this inner part and, if this loss is compensated by increased incidence, the outer parts may suffer a severe drag rise. The effect may be enhanced by the considerable modification in lift distribution, in comparison with that obtaining in the absence of interference effect. Thus, if this effect is not taken into account, a most careful aerodynamic calculation may become seriously invalidated, with a significant deterioration of performance.

A general three-dimensional theory of this phenomenon, covering arbitrary wing and body shapes, their relative positions, variable wing incidence, and compressibility, would be extremely complex and would require an unjustifiable amount of work. In the present paper, only the simplest possible

approach is attempted, based on two-dimensional flow of incompressible fluid, the wing being considered as a thin flat-plate aerofoil at zero incidence, and the body having a symmetrical oval shape with the axis of symmetry parallel to the wing (Fig. 8). The body may then be represented merely by a simple combination of sources and sinks in the presence of uniform flow. The coefficient of induced lift, and also the C.P. position, may be estimated by applying classical methods of two-dimensional hydrodynamics¹ involving conformal transformation and Kutta-Joukowski condition. The simplest case is a semi-infinite body obtained by using only a simple source (Figs. 1 and 2), and the simplest combination leading to a finite oval body consists of a single source and a single sink in a uniform flow. Only the above simplest cases are considered below, in Sections 1 and 2, respectively.

The theory of this paper presents many curious analogies with that of the rotating flap² and, in particular, many details of geometry and conformal transformation are common to both.

Acknowledgment is due to H. Barnes who has made computations and prepared the illustrations.

2. Case of Semi-Infinite Body.

2.1. Principles of the Method.

The simplest way of producing a non-lifting two-dimensional body is to combine a uniform flow (velocity V) with a single source, of strength Q , say (Fig. 1). This combination, as analysed in more detail in Appendix I, yields a semi-infinite body whose height tends asymptotically to

$$h = Q/V, \quad (1)$$

while the distance $SO = b$ between the stagnation point S and the source is:

$$b = Q/2\pi V = h/2\pi. \quad (2)$$

Let us suppose now that such a body is placed near and parallel to a very thin aerofoil LT (Fig. 2b) which is set at zero incidence. The flow must now be modified so as to make the aerofoil into a streamline, and this may be performed by the method of conformal transformation. We consider a circle of radius a in the auxiliary ζ -plane (Fig. 2a), and assume the aerofoil in 'physical' z -plane to be so thin that the conformal transformation is sufficiently approximated by the function:

$$z = \zeta + a^2/\zeta. \quad (3)$$

We then introduce a source of strength Q in Fig. 2a at a point:

$$\zeta_1 = \lambda a e^{i\varphi} \quad (4)$$

corresponding to the source at $z_1 = x_1 + iy_1$ in the physical plane. To make the circle into a streamline, we must¹ add the 'image' of the external source which consists of another source of strength $(+Q)$ at the image point:

$$\zeta_2 = \frac{a}{\lambda} e^{i\varphi} \quad (5)$$

and of a negative source (sink), of strength $(-Q)$, at the centre. Such a system of sources produces a flow indicated in Fig. 2a, symmetrical with respect to the line of sources, and there will be a certain finite velocity v_T at the point T corresponding to the trailing edge of the aerofoil. This

would give an infinite velocity at the trailing edge itself and, to avoid this and to satisfy Kutta-Joukowski condition, we must add a vortex at O, of negative circulation ($\Gamma = -\sigma Q$), the coefficient σ to be determined. The complex potential of the system, including all sources and the vortex, will be:

$$F_2(\zeta) = \frac{Q}{2\pi} \left\{ \ln \frac{(\zeta - \zeta_1)(\zeta - \zeta_2)}{\zeta} - i\sigma \ln \zeta \right\}, \quad (6a)$$

and the complex velocity in ζ -plane:

$$F_2'(\zeta) = \frac{Q}{2\pi} \left(\frac{1}{\zeta - \zeta_1} + \frac{1}{\zeta - \zeta_2} - \frac{1}{\zeta} - \frac{i\sigma}{\zeta} \right) = \frac{Q}{2\pi} \left\{ \frac{\zeta^2 - \zeta_1\zeta_2}{\zeta(\zeta - \zeta_1)(\zeta - \zeta_2)} - \frac{i\sigma}{\zeta} \right\}. \quad (6b)$$

The complex velocity in z -plane will be obtained by multiplying (6b) by

$$\frac{d\zeta}{dz} = \frac{\zeta^2}{\zeta^2 - a^2}, \quad (7)$$

in the form:

$$F_2'(\zeta) \frac{d\zeta}{dz} = \frac{Q}{2\pi} \frac{\zeta}{\zeta^2 - a^2} \left\{ \frac{\zeta^2 - \zeta_1\zeta_2}{(\zeta - \zeta_1)(\zeta - \zeta_2)} - i\sigma \right\}. \quad (8)$$

On the aerofoil itself, the velocity will be obtained by assuming that ζ corresponds to an arbitrary point on the circle, thus putting

$$\zeta = ae^{i\psi}, \quad (9)$$

and using (4) and (5):

$$F_2'(ae^{i\psi}) \frac{e^{2i\psi}}{e^{2i\psi} - 1} = \frac{Q}{4\pi a \sin \psi} \left\{ \frac{2 \sin(\varphi - \psi)}{\lambda + \frac{1}{\lambda} - 2 \cos(\varphi - \psi)} - \sigma \right\}. \quad (10)$$

This expression is real which proves that (6a) is a correct complex potential of a source in the presence of a rigid circular boundary. The Kutta-Joukowski condition now requires that $F_2'(a) = 0$, or that the expression in curly brackets in (10) should be 0 for $\psi = 0$. This leads to the basic formula for the 'circulation coefficient' σ :

$$\sigma = \frac{2 \sin \varphi}{\lambda + \frac{1}{\lambda} - 2 \cos \varphi}. \quad (11)$$

Since $\lambda + 1/\lambda \geq 2$, equation (11) shows that σ always has the same sign as $\sin \varphi$, i.e. the circulation Γ is negative or positive according as the body is above or below the wing.

The lift induced on the aerofoil, and the lift coefficient, are easily determined:

$$L_i \left(= C_{Li} \frac{\rho V^2}{2} c \right) = \rho V \Gamma = -\rho V Q \sigma, \quad (12)$$

$$C_{Li} = -\frac{2\sigma Q}{Vc} = -2\sigma \frac{h}{c}. \quad (13)$$

It will be interesting to consider a numerical example at this stage. In the case illustrated by Fig. 2, we have:

$$\lambda = 2.5, \quad \cos \varphi = 0.8, \quad \sin \varphi = 0.6, \quad \frac{x_1}{a} = 2.32, \quad \frac{y_1}{a} = 1.26, \quad h = 0.2c,$$

and hence:

$$\sigma = 0.923, \quad C_{Li} = -0.369.$$

The numerical value of C_{Li} obtained is quite considerable, and it is seen easily that even larger values are possible. A more detailed investigation of the variation of σ and C_{Li} with the relative position of aerofoil and body will be given in Section 2.3.

It must be mentioned that the shape of the body in Fig. 2b will differ somewhat from that in Fig. 1. The differences should be hardly perceptible, however, provided that h is not too large (i.e. that the body surface does not pass too close to the aerofoil).

2.2. Resultant Forces and Pitching Moments from Blasius Formulae.

The lift induced on the aerofoil has been already determined {form. (12)}, by simply applying the Kutta-Joukowski formula. It will be useful, however, to repeat the derivation by using Blasius formulae:

$$Y + iX = -\frac{1}{2}\rho \oint \{F'(\zeta)\}^2 \frac{d\zeta}{dz}, \quad (14a)$$

$$M = \frac{1}{2}\rho \Re e \left[\oint \{F'(\zeta)\}^2 \frac{d\zeta}{dz} z d\zeta \right], \quad (14b)$$

and this method will give us also the pitching moment M (about the origin). The complex velocity $F'(\zeta)$ will now be:

$$F'(\zeta) = F_1'(\zeta) + F_2'(\zeta) = V \left(1 - \frac{a^2}{\zeta^2} \right) + \frac{Q}{2\pi} \left(\frac{1}{\zeta - \zeta_1} + \frac{1}{\zeta - \zeta_2} - \frac{1 + i\sigma}{\zeta} \right). \quad (15)$$

The integrand in (14a), taking into account (7), becomes:

$$\begin{aligned} \{F'(\zeta)\}^2 \frac{d\zeta}{dz} &= V^2 \frac{\zeta^2 - a^2}{\zeta^2} + \frac{VQ}{\pi} \left(\frac{1}{\zeta - \zeta_1} + \frac{1}{\zeta - \zeta_2} - \frac{1 + i\sigma}{\zeta} \right) + \\ &+ \frac{Q^2}{4\pi^2} \frac{\zeta^2}{\zeta^2 - a^2} \left(\frac{1}{\zeta - \zeta_1} + \frac{1}{\zeta - \zeta_2} - \frac{1 + i\sigma}{\zeta} \right)^2, \end{aligned} \quad (16)$$

and the integration may be performed along appropriate contours in ζ -plane, to give the resultant forces acting on the aerofoil, body, or the entire system, respectively. Considering the entire system first, we have to determine the residue of the integrand with respect to the pole at infinity ($\zeta = \infty$). The residues of the first and third terms are obviously zero, that of the second term is:

$$\frac{VQ}{\pi} (1 + 1 - 1 - i\sigma),$$

and hence:

$$\begin{aligned} Y_S + iX_S &= -\frac{1}{2}\rho 2\pi i \frac{VQ}{\pi} (1 - i\sigma) = -\rho VQ(\sigma + i), \\ Y_S &= -\rho VQ\sigma, \quad X_S = -\rho VQ. \end{aligned} \quad (17)$$

Thus, we have found Y_S equal to L_i , as could be expected. As to X_S , we may guess this to be the resultant force acting on the body. This guess is confirmed by performing the integration (14a) along a contour enclosing only the pole ζ_1 . The residue of the 2nd term in (16) is then VQ/π , and hence we obtain:

$$Y_B = 0, \quad X_B = -\rho VQ. \quad (18)$$

As a check, we may still perform the integration (14a) along the circle, i.e. taking residues with respect to the poles 0 and ζ_2 ; the result is:

$$Y_A = -\rho VQ\sigma, \quad X_A = 0. \quad (19)$$

The resultant ‘forward thrust’ on the body, shown by (18), may cause some doubts. However, the same result is obtained for the simple case of a semi-infinite body shown in Fig. 1, taken alone. In that case, the momentum of the entire fluid (outside and inside the body) increases by ρVQ per unit time owing to the presence of the source, so that the body should exert on the fluid a force of the same amount in the direction of flow, and the body should be subject to an equal force of opposite sign*.

The first term in (16) will give no force on either aerofoil or body, but the third term will lead to additional forces on both, proportional to ρQ^2 . As the corresponding force on the system is nil, they must be equal and opposite, and should be considered as internal forces in the system. They may be calculated by evaluating the appropriate residues, but there is no point in giving here the respective (rather complicated) formulae, especially as these internal forces are quite small generally.

To calculate the *pitching moments*, we use (14b), and the new integrand will be obtained by multiplying the previous one (16) by (3), so it becomes:

$$\begin{aligned} \{F'(\zeta)\}^2 \frac{d\zeta}{dz} z &= V^2 \frac{\zeta^4 - a^4}{\zeta^3} + \frac{VQ}{\pi} \left\{ \frac{\zeta^2 + a^2}{\zeta(\zeta - \zeta_1)} + \frac{\zeta^2 + a^2}{\zeta(\zeta - \zeta_2)} - (1 + i\sigma) \frac{\zeta^2 + a^2}{\zeta^2} \right\} + \\ &+ \frac{Q^2}{4\pi^2} \frac{\zeta(\zeta^2 + a^2)}{\zeta^2 - a^2} \left(\frac{1}{\zeta - \zeta_1} + \frac{1}{\zeta - \zeta_2} - \frac{1 + i\sigma}{\zeta} \right)^2. \end{aligned} \quad (20)$$

Considering again the entire system first, we find the residue of the second term with respect to $\zeta = \infty$ to be:

$$\frac{VQ}{\pi} (\zeta_1 + \zeta_2) = \frac{VQa}{\pi} \left(\lambda + \frac{1}{\lambda} \right) e^{i\varphi}, \quad (21)$$

and hence the pitching moment on the system:

$$M_S = \frac{\rho}{2} \mathcal{H}e \left\{ 2VQa \left(\lambda + \frac{1}{\lambda} \right) (i \cos \varphi - \sin \varphi) \right\} = -\rho VQa \left(\lambda + \frac{1}{\lambda} \right) \sin \varphi. \quad (22)$$

This may be considered as a sum of moments of the forces X_B and Y_A about the origin. The force X_B , given by (18), acts presumably along the horizontal line through the source z_1 , so its moment is found as:

$$M_B = X_B y_1 = -\rho VQa \left(\lambda - \frac{1}{\lambda} \right) \sin \varphi, \quad (23)$$

and hence the moment of the force Y_A becomes $M_A = M_S - M_B$, or:

$$M_A = -\rho VQa \frac{2 \sin \varphi}{\lambda}. \quad (24)$$

These results may be checked, by evaluating the residue of the second term of (20) with respect to the pole ζ_1 :

$$\frac{VQ}{\pi} \frac{\zeta_1^2 + a^2}{\zeta_1} = \frac{VQ}{\pi} \left(\lambda e^{i\varphi} + \frac{1}{\lambda} e^{-i\varphi} \right), \quad (25)$$

* If the body is considered as a solid, no new momentum is created, and there will be no thrust. The matter has little significance for our problem, as the body must in reality be always a finite closed one, and then there will be sources and sinks, with the sum total of their strengths always zero, and no resultant thrust or drag will appear.

which leads directly to (23); or by evaluating the residues with respect to the poles ζ_2 and 0:

$$\frac{VQ}{\pi} \frac{\zeta_2^2 + a^2}{\zeta_2}, \quad \text{and} \quad -\frac{VQ}{\pi} \left(\frac{a^2}{\zeta_1} + \frac{a^2}{\zeta_2} \right), \quad (26)$$

respectively, which bring us back to (24).

The *centre of pressure* of the induced lift L_i (or Y_A) will be determined by its distance na ahead of the origin, where:

$$n = \frac{M_A}{Y_A a} = \frac{2 \sin \varphi}{\lambda \sigma} = \frac{1}{\lambda} \left(\lambda + \frac{1}{\lambda} - 2 \cos \varphi \right), \quad (27)$$

or by its distance $H_A c$ behind the leading edge, where:

$$H_A = (50 - 25n)\%. \quad (28)$$

Considering the numerical example given in Section 2.1, we obtain $n = 0.52$, $H_A = 37\%$.

2.3. Variation of Induced Lift with Body Position and Size.

The circulation coefficient σ , given by form. (11), depends only on λ and φ , i.e. on the position of the external source. A good illustration is obtained by determining loci of constant σ in the physical plane. These loci can be found by using their parametric equations:

$$\frac{x_1}{a} = \left(\lambda + \frac{1}{\lambda} \right) \cos \varphi, \quad \frac{y_1}{a} = \left(\lambda - \frac{1}{\lambda} \right) \sin \varphi, \quad (29)$$

where, according to (11):

$$\lambda + \frac{1}{\lambda} = 2 \left(\cos \varphi + \frac{\sin \varphi}{\sigma} \right). \quad (30)$$

A number of such loci are shown in Fig. 3, for several values of σ . All loci issue from the trailing edge and are symmetrical with respect to the x -axis, but the upper halves correspond to anti-clockwise circulation, and *vice versa*. The very high values of σ , appearing in the near vicinity of the trailing edge, have little significance because, for such positions, the possible ratio h/c would be very small, and hence the values of C_{Li} , from (13), not particularly large.

The formula (11) is not very convenient, as it gives σ in terms of co-ordinates in the ζ -plane. It can be transformed, however, and presented simply in terms of 'bi-polar' co-ordinates d_1 , d_2 in the physical plane (Fig. 2b). Using (29), we obtain:

$$d_1 = \sqrt{\{(x_1 + 2a)^2 + y_1^2\}} = a \left(\lambda + \frac{1}{\lambda} + 2 \cos \varphi \right) \text{ and, similarly: } d_2 = a \left(\lambda + \frac{1}{\lambda} - 2 \cos \varphi \right), \quad (31)$$

hence:

$$\lambda + \frac{1}{\lambda} = 2 \frac{d_1 + d_2}{c}, \quad \cos \varphi = \frac{d_1 - d_2}{c}, \quad (32)$$

so that (11) and (13) become:

$$\sigma = \pm \frac{\sqrt{\{c^2 - (d_1 - d_2)^2\}}}{2d_2}, \quad (33)$$

$$C_{Li} = \mp \frac{h \sqrt{\{c^2 - (d_1 - d_2)^2\}}}{cd_2}, \quad (34)$$

where the upper and lower signs correspond to the source being situated in the upper and lower half-plane respectively.

Coming back to Fig. 3, it is seen that when moving along any horizontal line parallel to the aerofoil, from $x = -\infty$ to $x = +\infty$, σ first increases from 0 to a certain maximum and then falls back to 0, the maximum corresponding to the point of contact with one of the loci $\sigma = \text{const.}$ — This is illustrated better by Fig. 4 which gives several curves showing variation of σ along such lines (note shift of scales of σ for particular curves). The equation of each curve may be obtained in a convenient form by transforming (33) so as to eliminate d_1 , d_2 and introducing instead y_1 and the angle β (Fig. 2b). We have:

$$d_2 = y_1 \operatorname{cosec} \beta, \quad d_1^2 = c^2 + 2cy_1 \cot \beta + y_1^2 \operatorname{cosec}^2 \beta \quad (35)$$

and hence, after some transformation:

$$2y_1\sigma^2 = \sqrt{\{c^2 \sin^2 \beta + 2cy_1 \sin \beta \cos \beta + y_1^2\}} - c \sin \beta \cos \beta - y_1. \quad (36)$$

Equating to 0 the first derivative of (36) with respect to β (y_1 being considered constant), and simplifying, we obtain the condition for maxima in the form:

$$\frac{\cos 4\beta_m - \cos 2\beta_m}{2 \sin 4\beta_m} = \frac{y_1}{c}, \quad (37)$$

and the expression for σ_{\max} :

$$\sigma_{\max}^2 = \frac{\cos^2 2\beta_m - 1}{2 \cos 2\beta_m + 1}. \quad (38)$$

It is easily found that $90^\circ < \beta_m < 120^\circ$, the larger angles corresponding to smaller values of y_1/c . The characteristic values for the curves of Fig. 4 are tabulated below {including $(-C_{Li})_{\max}$ calculated from form. (13) assuming that $h = y_1$, i.e. allowing a generous gap between aerofoil and body}.

y_1/a	β_m°	σ_{\max}	x_1/a	$(-C_{Li})_{\max}$, for $h = y_1$
0.5	117.46	2.117	1.740	0.529
1.0	114.74	1.389	1.539	0.695
1.5	112.05	1.054	1.392	0.790
2.0	109.57	0.850	1.289	0.850

It is seen that surprisingly big values of C_{Li} seem attainable and that although σ_{\max} decreases with rising y_1/a , $(-C_{Li})_{\max}$ increases if the body thickness is allowed to rise in proportion.

The curve 'C' in Fig. 4 is the locus of points for which σ assumes maximum values along the horizontals.

If the source is near the aerofoil trailing edge (d_2 small compared with c) then the formula (33) can be transformed, eliminating d_1 , introducing instead the 'polar angle' β (Fig. 2b), and expanding into a power series. We obtain:

$$d_1 = \sqrt{\left\{ (c+d_2)^2 - 4cd_2 \sin^2 \frac{\beta}{2} \right\}} = c + d_2 - \frac{2cd_2}{c+d_2} \sin^2 \frac{\beta}{2} - \frac{2c^2d_2^2}{(c+d_2)^3} \sin^4 \frac{\beta}{2} - \frac{4c^3d_2^3}{(c+d_2)^5} \sin^6 \frac{\beta}{2} \dots,$$

$$c^2 - (d_1 - d_2)^2 = \frac{4c^2d_2}{c+d_2} \sin^2 \frac{\beta}{2} \left\{ 1 - \frac{d_2^2}{(c+d_2)^2} \sin^2 \frac{\beta}{2} - \frac{2cd_2^3}{(c+d_2)^4} \sin^4 \frac{\beta}{2} \dots \right\},$$

and finally:

$$\sigma = \frac{c}{\sqrt{\{d_2(c+d_2)\}}} \sin \frac{\beta}{2} \left\{ 1 - \frac{d_2^2}{2(c+d_2)^2} \sin^2 \frac{\beta}{2} - \frac{d_2^3(c+d_2/8)}{(c+d_2)^4} \sin^4 \frac{\beta}{2} \dots \right\}. \quad (39)$$

The series converges so well when the ratio d_2/c is small that it may often suffice to neglect all but the first term. The convergence is satisfactory even when d_2/c is not so small. Considering the numerical example of Section 2.1, we have, using (31):

$$\frac{d_1}{a} = 4.5, \quad \frac{d_2}{a} = 1.3, \quad \cos \beta = \frac{(\lambda^2 + 1) \cos \varphi - 2\lambda}{\lambda^2 + 1 - 2\lambda \cos \varphi} = 0.24615;$$

$$\sin \frac{\beta}{2} = \frac{\lambda + 1}{\sqrt{(\lambda^2 + 1 - 2\lambda \cos \varphi)}} \sin \frac{\varphi}{2} = 0.61394$$

and, from (39):

$$\sigma = 0.93557(1 - 0.01134 - 0.00165 \dots);$$

three consecutive approximations are 0.936, 0.925, 0.923, the first one being reasonably accurate, and the last one having three exact decimals.

Introducing (39) into (13), while keeping only the first term of the series, we obtain the very simple approximate formula for the lift coefficient:

$$C_{Li} \approx - \frac{2h}{\sqrt{\{d_2(c + d_2)\}}} \sin \frac{\beta}{2}. \quad (40)$$

2.4. Variation of Centre of Pressure with Body Position.

The position of centre of pressure of the induced lift is given in terms of the co-ordinates λ, φ by (27, 28). A good illustration is obtained again by determining loci of constant n or H_A in the physical plane. Their parametric equations will be:

$$\frac{x_1}{a} = \left(\lambda + \frac{1}{\lambda} \right) \cos \varphi, \quad \frac{y_1}{a} = \left(\lambda - \frac{1}{\lambda} \right) \sin \varphi, \quad (41)$$

where, according to (27):

$$\cos \varphi = \frac{1 - n}{2} \lambda + \frac{1}{2\lambda}. \quad (42)$$

A number of such loci are shown in Fig. 5, for several values of n (or H_A). It is found that $4 > n > 0$, thus $-50\% < H_A < +50\%$, the limiting values corresponding to the leading and trailing edge, respectively. The centre of pressure lies usually in the front half of the aerofoil, except the positions of the source enclosed by the small locus ($n = 2, H_A = 0\%$), for which the C.P. lies forward of the leading edge.

It will be convenient to have the C.P. position expressed in terms of co-ordinates d_1, d_2 in the physical plane. Using (31), we obtain from (27):

$$n = \frac{4d_2}{d_1 + d_2 + \sqrt{\{(d_1 + d_2)^2 - c^2\}}}. \quad (43)$$

3. Case of a Finite Body of Oval Shape.

3.1. Theory and General Discussion.

A simple finite two-dimensional body of oval cross-section is obtained by combining uniform flow with a source and a sink of equal strength (Q), as analysed in more detail in Appendix II, and illustrated in Figs. 6 and 7.

If such a body is placed near and parallel to a thin aerofoil set at zero incidence (Fig. 8), then the flow may be represented, with fair accuracy, in a way analogous to that applied in Section 2.1.

The only difference is that, instead of one source, there will be one positive and one negative source in the auxiliary plane, at ζ_1 and ζ_1' , respectively, together with their images and associated vortices at the centre of the circle. The respective circulations will be $(-\sigma Q)$ and $(+\sigma' Q)$, where σ and σ' can be determined from (11) or (33) by substituting the co-ordinates of the respective sources. The lift induced on the aerofoil, and the lift coefficient, will now be:

$$L_i \left(= C_{Li} \frac{\rho V^2}{2} c \right) = -\rho V Q (\sigma - \sigma') \quad (44)$$

and

$$C_{Li} = -\frac{2Q(\sigma - \sigma')}{Vc} \quad (45)$$

or, taking into account form. (72) of Appendix II:

$$C_{Li} = -2(\sigma - \sigma') \frac{h}{c} \mu. \quad (46)$$

The centre-of-pressure position will be obtained in the usual way as for two parallel and opposite forces. Its distance ahead of the origin will be n^*a , where:

$$n^* = \frac{\sigma n - \sigma' n'}{\sigma - \sigma'}, \quad (47)$$

n and n' to be determined from (27) or (43).

It must be mentioned that formulae (46, 47) can only be used when the axis of the body is parallel to the aerofoil, so that $y_1 = y_1'$, or

$$\left(\lambda - \frac{1}{\lambda} \right) \sin \varphi = \left(\lambda' - \frac{1}{\lambda'} \right) \sin \varphi'. \quad (48)$$

Let us suppose now that we have to deal with an oval body of the shape corresponding approximately to that of Fig. 6, and that only its basic dimensions L , h , and the position relative to the aerofoil, are known. Then Appendix II and the numerical table therein permit determination of the positions of both sources z_1 , z_1' , by evaluating the ratio e/h corresponding to the thickness ratio $\vartheta = h/L$. Hence any convenient co-ordinates of the sources can be found. The table also supplies values of the coefficient μ which is needed for using the formula (46). These parameters can also be read off the diagram in Fig. 7.

Studying the basic formula (46), we see that, for the induced-lift coefficient to become large, the essential condition is not that both σ and σ' are large, but that their difference $(\sigma - \sigma')$ acquires as big a value as possible. Considering Fig. 4, we notice that, if the centre of the oval is at, or near, the point corresponding to σ_{\max} on any of the horizontal lines, then σ and σ' will be nearly equal, so that C_{Li} will nearly vanish. To obtain the greatest possible negative value of C_{Li} , it will be necessary to place the centre of the oval at, or near, the point corresponding to *maximum negative slope* of the appropriate σ -curve in Fig. 4. This is so, at least, for comparatively short ovals.

We also notice the interesting (perhaps surprising) fact that, if the oval is moved sufficiently forward, we may have $\sigma < \sigma'$, and then C_{Li} will *change sign*, becoming positive when the oval lies above the aerofoil. To obtain large numerical values for a comparatively short oval, the body centre should be placed near the point corresponding to *maximum positive slope* of the appropriate σ -curve in Fig. 4.

If, finally, the oval body is of considerable length (say of the order of the aerofoil chord), then the biggest effect will occur when the front source is on, or near, the curve C in Fig. 4, i.e. in conditions similar to those of the semi-infinite body. This is so because σ' will then be negligibly small, so σ must be as large as possible.

The curve 'i' in Fig. 4 is an approximate locus of points corresponding to maximum negative slopes of σ -curves.

3.2. Numerical Example.

In Fig. 8, the source is located exactly at the same point as in Fig. 2, so that:

$$\lambda = 2.5, \quad \sin \varphi = 0.6, \quad \cos \varphi = 0.8, \quad \frac{x_1}{a} = 2.32, \quad \frac{y_1}{a} = 1.26, \quad \sigma = 0.923, \quad n = 0.520.$$

For the sink, we have assumed:

$$\lambda' = 4, \quad \sin \varphi' = 0.336, \quad \cos \varphi' = 0.94186,$$

so that

$$\frac{x_1'}{a} = 4.0029, \quad \frac{y_1'}{a} = 1.26, \quad \sigma' = 0.284, \quad n' = 0.592$$

(it is seen that $y_1' = y_1$). The shape of the oval is assumed to be the same as in Fig. 6, i.e. corresponding to

$$\eta_m = 2.5.$$

Formulae (67 to 72) of Appendix II then give:

$$\gamma = 7.524, \quad \xi_s = 8.465, \quad \vartheta = 0.295, \quad \mu = 1.257,$$

then:

$$\frac{h}{c} = \frac{x_1' - x_1}{c} \frac{\eta_m}{\gamma} = 0.1398$$

and, finally, from (46, 47), we find:

$$C_{Li} = -0.225, \quad n^* = 0.488 \quad (H_A^* = 37.8\%).$$

It is obvious that appreciably larger values of C_{Li} are obtainable, by choosing larger ovals in appropriate positions.

4. Concluding Remarks.

The theory of the preceding sections gives complete answers as to the magnitude of the induced lift and its C.P. position, but only within a restrictive range of rather narrow assumptions. The question arises how far can this crude theory be useful in practical cases, apart from general qualitative understanding of the subject. A full answer can probably be given only by experiments. It may be worthwhile, however, to consider briefly the major factors which can influence the phenomenon and cause deviations from our results.

(1) While the effect of the front source is probably estimated correctly, that of the sink in the rear may become considerably blurred and reduced because of the wake behind the body. This may not be important when the sink is far back (so that σ' is small anyhow), but may change the results considerably in the opposite case. It seems therefore unlikely that considerable positive C_{Li} could be obtained with the body in forward position.

(2) The shape of the body chosen in our investigation was somewhat accidental (caused by the tendency to keep the theory as simple as possible), and the only variable parameter was the thickness ratio. It would not be very difficult to consider alternative shapes, by introducing more sources and sinks, or continuous source distributions. The results should not differ much from ours, however.

(3) In the present paper, only the case of body and wing at zero incidence was considered. The results should not be altered much in the case of wing and body at small incidence, but it would be difficult to estimate this effect.

(4) If the non-lifting body is an engine nacelle, then it cannot be considered as an impenetrable obstacle to the relative wind, as assumed throughout in this paper; the lift-producing capacity may therefore be considerably decreased.

(5) The most important cause of discrepancies will be, of course, that a 2-dimensional theory is never able to predict quantitative results for 3-dimensional bodies and systems reliably. There are several features to be considered. Even in the case of a wing of large aspect ratio, the external bodies (nacelles) will never occupy the whole of the span. Each nacelle is likely to resemble a body of revolution, rather than a transverse oblong oval cylinder. And, finally, the wing may have various plan-forms, with sweepback, taper, etc.—An attempt to deal theoretically with such problems would encounter formidable difficulties. It is clear, however, that there will be many contributory causes to reduce the induced lift, often to a mere fraction of what would apply in a 2-dimensional system. If, however, we had something like a row of four or six nacelles occupying a considerable part of the wing span, then this central part might be subject to an incremental local lift only little smaller than that predicted for two dimensions, while the outer parts would remain almost unaffected.

(6) The above factors tend mostly to reduce the induced-lift effects. However, compressibility at high subsonic Mach numbers may increase them considerably, as has been already shown experimentally. It is in such conditions where these effects may play a particularly important part.

SYMBOLS

a	Radius of basic circle (Fig. 2a)
b	Length defined by (2)
C_{Li}	Coefficient of induced lift
c	$= 4a$, chord of aerofoil (Fig. 2b)
d_1, d_2	Distances from source to L.E. and T.E. of aerofoil (Fig. 2b)
e	Distance from source to foremost point of oval body (Fig. 8)
$F(\zeta)$	Complex potential in ζ -plane
$F_1(\zeta)$	Part of $F(\zeta)$ representing undisturbed flow past circle
$F_2(\zeta)$	Part of $F(\zeta)$ due to external body
H_A	Distance of C.P. of induced lift, aft of L.E. of aerofoil, expressed as fraction of chord, in %
L	Length of body
L_i	Induced lift
l	Distance from body centre to source (Fig. 6)
M	Pitching moment about origin (mid-chord axis)
n	Distance of C.P. of induced lift, ahead of mid-chord, expressed as a fraction of radius a
Q	Strength of source
$\Re e$	Real part of a complex quantity
r	Radius vector in Appendix I
V	Velocity of undisturbed uniform flow
X, Y	Force components in physical plane
z	$= x + iy$, complex co-ordinate in physical plane (Fig. 2b); also in Appendix II (Fig. 6)
z_1	$= x_1 + iy_1$, complex co-ordinate of source in physical plane
β	Angle (Fig. 2b)
Γ	Circulation of vortex at centre of circle, or corresponding circulation round aerofoil
γ	See (64)

SYMBOLS—*continued*

ζ	Complex co-ordinate in auxiliary plane (Fig. 2a)
ζ_1, ζ_2	Complex co-ordinates of sources in auxiliary plane (Fig. 2a)
Φ, Ψ	Velocity potential and stream function
φ	Polar angle of sources
ψ	Polar angle of a point on circle
ξ, η	Non-dimensional co-ordinates (Fig. 6)
ξ_s	Value of ξ at stagnation point S_2 (Fig. 6)
η_m	Maximum η for oval (Fig. 6)
ϑ	Thickness ratio of body
θ	Polar angle in Appendix I
λ	Radius vector of source (Fig. 2a) expressed as multiple of a
μ	Ratio defined by (72)
ρ	Air density
$\sigma =$	$-\Gamma/Q$, circulation coefficient

Suffices

s	System
A	Aerofoil
B	Body

REFERENCES

<i>No.</i>	<i>Author</i>	<i>Title, etc.</i>
1	L. M. Milne-Thomson ..	<i>Theoretical hydrodynamics</i> . Paras. 8.21 and 8.61, Macmillan & Co., London, 1938.
2	S. Neumark	Two-dimensional theory of an aerofoil with a rotating flap. R.A.E. Report Aero. 2641. A.R.C. 22,540. July, 1960. Also: Rotating aerofoils and flaps. <i>J. R. Ae. S.</i> , Vol. 67. January, 1963.

APPENDIX I

Semi-Infinite Body in Two Dimensions

The complex potential and velocity of a combination of uniform flow with a single source (Fig. 1) can be written:

$$f(z) = \Phi + i\Psi = Vz + \frac{Q}{2\pi} \ln z, \quad (49)$$

$$f'(z) = v_x - iv_y = V + Q/2\pi z. \quad (50)$$

The only stagnation point S is obtained equating (50) to zero:

$$z_s = -Q/2\pi V = -b, \quad \text{say.} \quad (51)$$

Introducing polar co-ordinates defined by

$$z = re^{i\theta}, \quad (52)$$

we may write the stream function Ψ in the form:

$$\Psi = V\{r \sin \theta - b(\pi - \theta)\}, \quad (53)$$

and it is seen then that $\Psi = 0$ at the stagnation point, so that the equation of the profile is:

$$y = r \sin \theta = b(\pi - \theta). \quad (54)$$

For $\theta \rightarrow 0$, or $\theta \rightarrow 2\pi$, we have $y \rightarrow \pm \pi b$, so there are two horizontal asymptotes, and the height (thickness) of the body, reckoned from one asymptote to another, is:

$$h = 2\pi b. \quad (55)$$

The general equation of other streamlines is given by (54) which can be written

$$r \sin \theta = b\{\pi(1+p) - \theta\}, \quad (56)$$

where

$$p = \Psi/\pi Vb \quad (57)$$

is a convenient parameter. Several streamlines are shown in Fig. 1.

APPENDIX II

Finite Body of Oval Shape in Two Dimensions

Let us consider a combination of uniform flow with one positive and one negative source, at $z = \pm l$, respectively (Fig. 6). Denoting the strength of either source by

$$Q = 2\pi Vb, \quad (58)$$

we may write the complex potential and velocity in the form:

$$f(z) = \Phi + i\Psi = Vz + \frac{Q}{2\pi} \ln \frac{z+l}{z-l} = V \left(z + b \ln \frac{z+l}{z-l} \right), \quad (59)$$

$$f'(z) = v_x - iv_y = V \left(1 - \frac{2bl}{z^2 - l^2} \right). \quad (60)$$

There are two stagnation points S_1, S_2 on x -axis, obtained by equating (60) to zero:

$$z_s = x_s = \pm \sqrt{l^2 + 2bl}, \quad y_s = 0. \quad (61)$$

The stream function Ψ may be written:

$$\Psi = V \left(y - b \tan^{-1} \frac{2ly}{x^2 + y^2 - l^2} \right), \quad (62)$$

and then $\Psi = 0$ at the stagnation points, and hence on the profile.

It is convenient to introduce non-dimensional co-ordinates:

$$\xi = x/b, \quad \eta = y/b, \quad (63)$$

and a non-dimensional parameter:

$$\gamma = l/b. \quad (64)$$

The stream function then becomes:

$$\Psi = Vb \left(\eta - \tan^{-1} \frac{2\gamma\eta}{\xi^2 + \eta^2 - \gamma^2} \right), \quad (65)$$

and the equation of the profile ($\Psi = 0$):

$$\xi^2 = \gamma^2 - \eta^2 + 2\gamma\eta \cot \eta. \quad (66)$$

We have therefore a family of ovals (with one variable parameter γ), varying from a circle (for $\gamma = 0$) to a semi-infinite shape (for $\gamma = \infty$). For stagnation points we obtain:

$$\xi_s^2 = \gamma^2 + 2\gamma, \quad (67)$$

and for the vertices on y -axis:

$$\gamma^2 + 2\gamma\eta_m \cot \eta_m - \eta_m^2 = 0, \quad \text{whence} \quad \gamma = \eta_m \tan \frac{\eta_m}{2}. \quad (68)$$

The length and thickness of the oval will be

$$L = 2b\xi_s, \quad h = 2b\eta_m, \quad (69)$$

and the thickness ratio:

$$\vartheta = h/L = \eta_m/\xi_s. \quad (70)$$

The formulae (67, 68, 70) relate all relevant geometric parameters γ , ξ_s , η_m and ϑ to each other. Two additional parameters, needed for the theory of Section 3, are:

(1) the ratio of the distance e (between the source and the stagnation point) to the thickness h :

$$\frac{e}{h} = \frac{\xi_s - \gamma}{2\eta_m}, \quad \text{and} \quad (71)$$

(2) the ratio

$$\mu = Q/Vh = \pi/\eta_m. \quad (72)$$

In the case of a semi-infinite body we had $e/h = 1/2\pi = 0.1592$, $\eta_m = \pi$, $\mu = 1$. For finite ovals, these parameters assume varying values.

The easiest way to tabulate the above parameters is to choose a number of values for η_m , and to work out the remaining ones. However, if we have an oval body resembling that of Fig. 6, with unknown parameters, the only one easily determined is the thickness ratio ϑ . The following table (easily interpolated) gives the values of all parameters for a number of round values of ϑ .

ϑ	η_m	γ	ξ_s	e/h	μ	
0	3.1416	∞	∞	0.1592	1	semi-infinite body
0.05	3.0400	59.802	60.794	0.1631	1.0334	
0.10	2.9354	28.371	29.354	0.1674	1.0702	
0.15	2.8279	17.880	18.853	0.1721	1.1109	
0.20	2.7176	12.627	13.590	0.1772	1.1560	
0.25	2.6046	9.466	10.418	0.1828	1.2062	
0.30	2.4891	7.358	8.297	0.1888	1.2621	
0.35	2.3712	5.848	6.775	0.1954	1.3249	
0.40	2.2509	4.715	5.627	0.2026	1.3957	
1	0	0	0	0.5	∞	circle

In Fig. 7, η_m , e/h and μ are plotted against ϑ .

The general equation of streamlines is given by (65) which can be written:

$$\xi^2 = \gamma^2 - \eta^2 + 2\gamma\eta \cot(\eta - \pi p), \quad (73)$$

where

$$p = \Psi/\pi Vb. \quad (74)$$

Several streamlines are shown in Fig. 6.

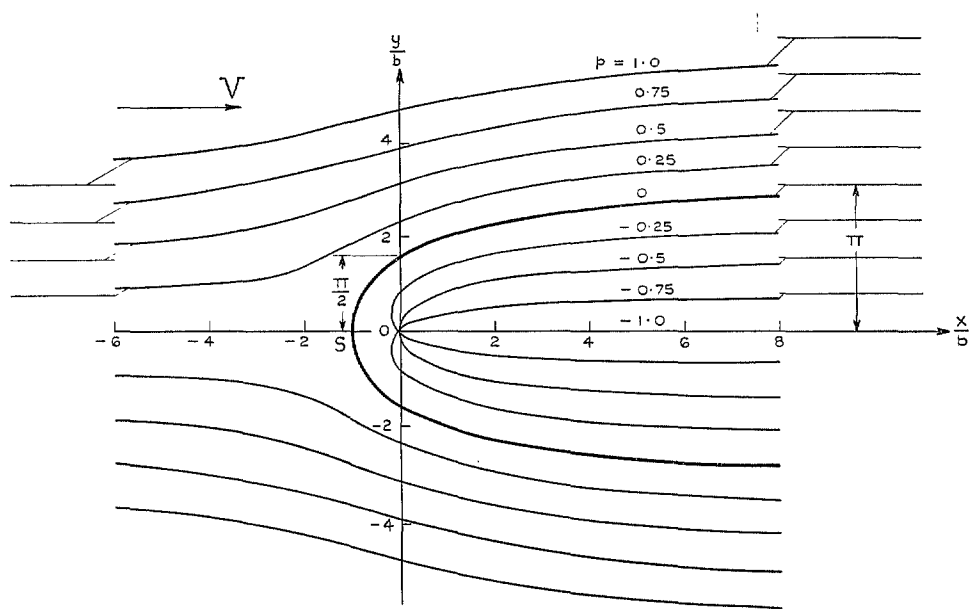


FIG. 1. Semi-infinite body obtained by combining uniform flow and single source.

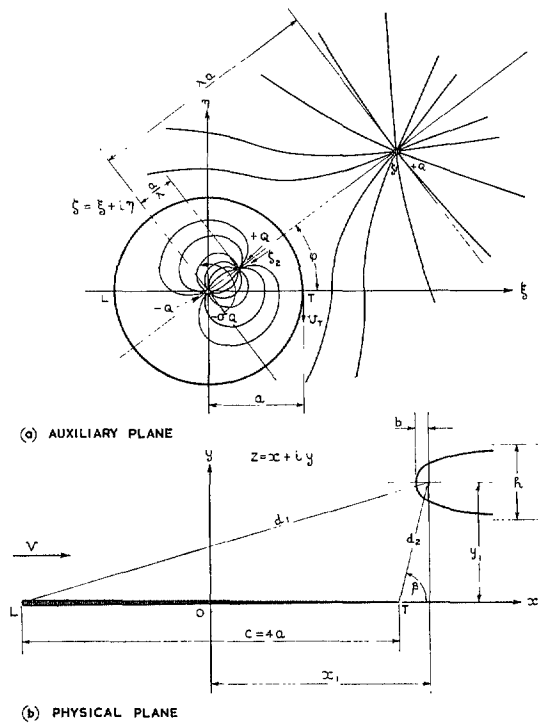


FIG. 2. Aerofoil and semi-infinite body. Conformal transformation.

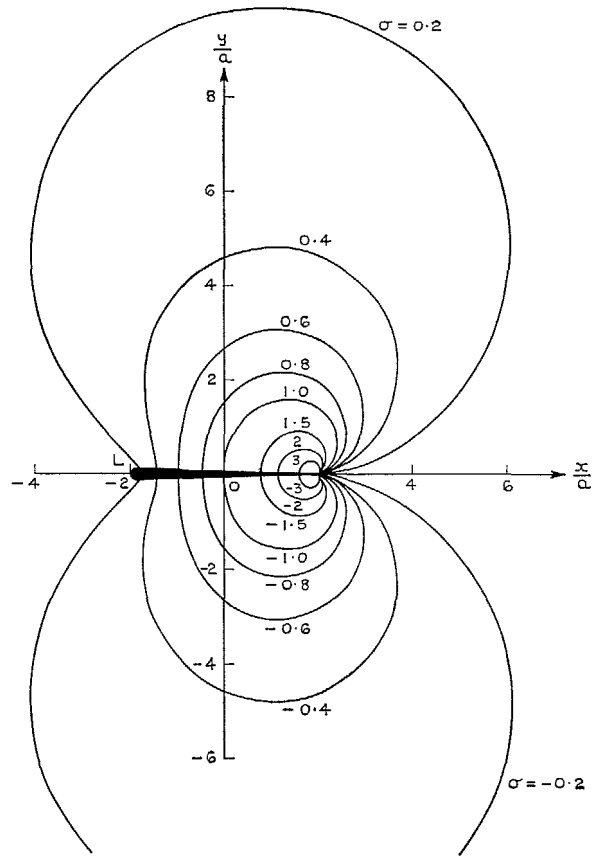


FIG. 3. Circulation induced by semi-infinite body. Loci of constant σ in physical plane.

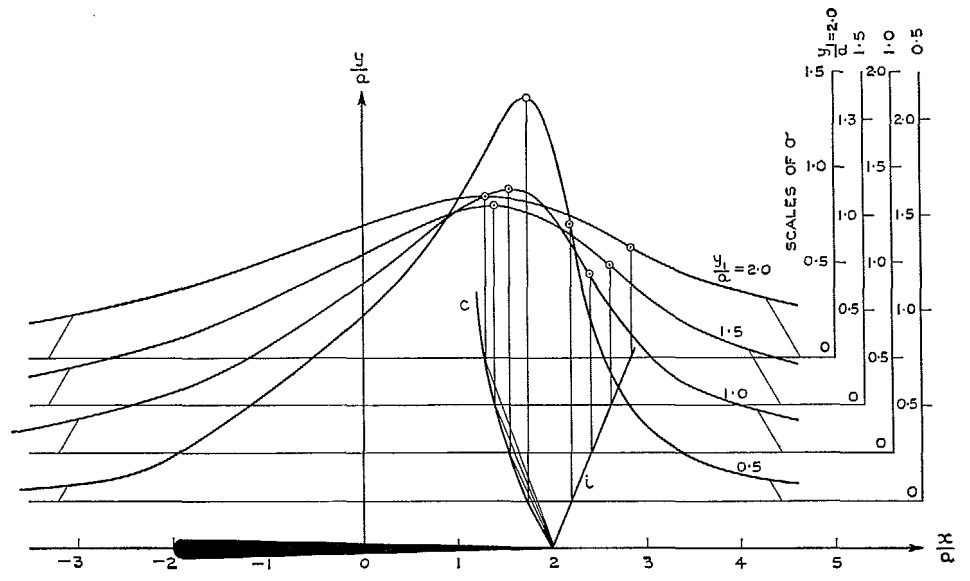


FIG. 4. Circulation induced by semi-infinite body. Variation of σ along horizontals.

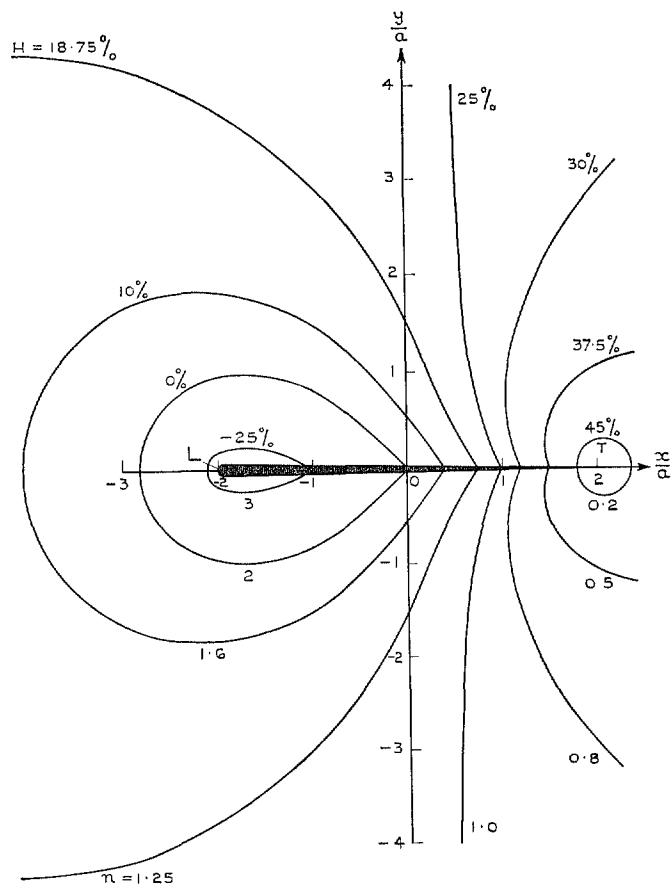


FIG. 5. Lift induced on aerofoil by semi-infinite body.
Loci of source centres for constant C.P. positions.

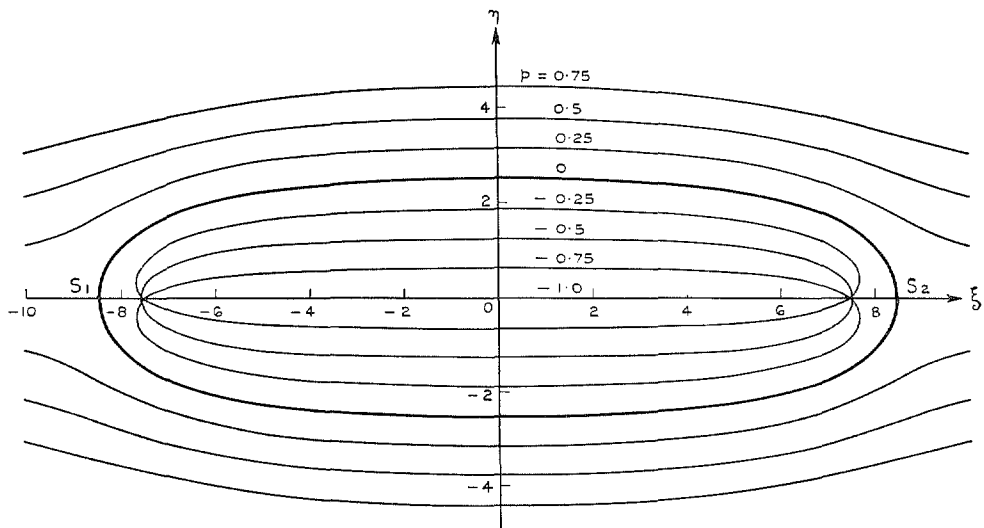


FIG. 6. Finite body obtained by combining uniform flow, one source and one sink.

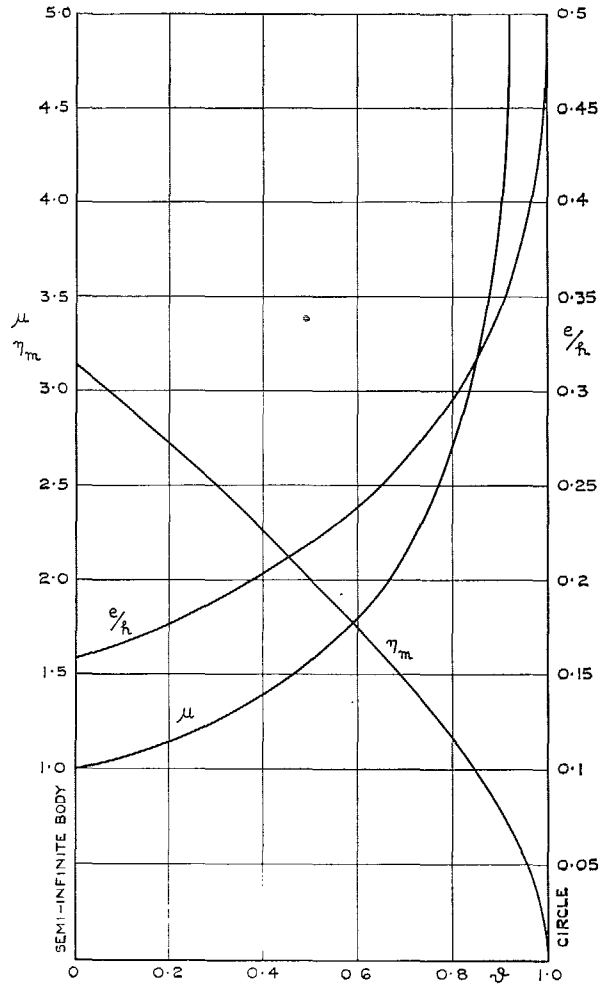


FIG. 7. Characteristic parameters of finite oval body.

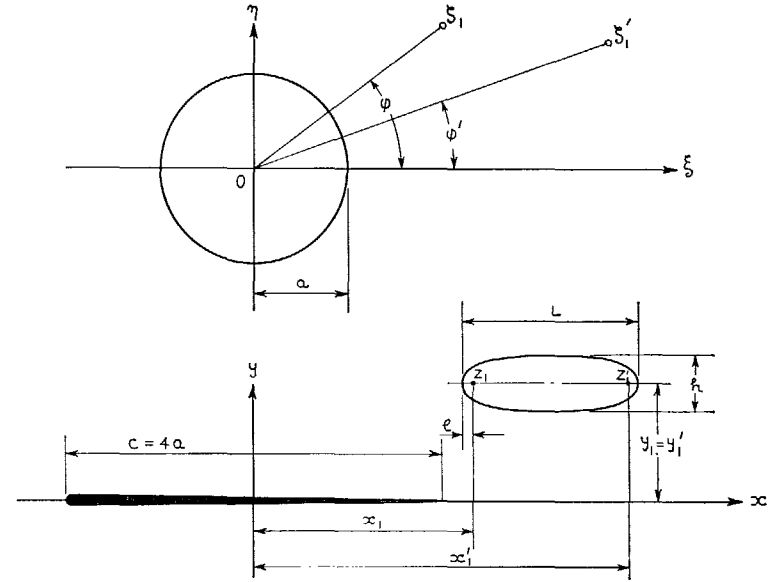


FIG. 8. Aerofoil and finite body of oval shape.

Publications of the Aeronautical Research Council

ANNUAL TECHNICAL REPORTS OF THE AERONAUTICAL RESEARCH COUNCIL (BOUND VOLUMES)

- 1945 Vol. I. Aero and Hydrodynamics, Aerofoils. £6 10s. (£6 13s. 6d.)
Vol. II. Aircraft, Airscrews, Controls. £6 10s. (£6 13s. 6d.)
Vol. III. Flutter and Vibration, Instruments, Miscellaneous, Parachutes, Plates and Panels, Propulsion. £6 10s. (£6 13s. 6d.)
Vol. IV. Stability, Structures, Wind Tunnels, Wind Tunnel Technique. £6 10s. (£6 13s. 3d.)
- 1946 Vol. I. Accidents, Aerodynamics, Aerofoils and Hydrofoils. £8 8s. (£8 11s. 9d.)
Vol. II. Airscrews, Cabin Cooling, Chemical Hazards, Controls, Flames, Flutter, Helicopters, Instruments and Instrumentation, Interference, Jets, Miscellaneous, Parachutes. £8 8s. (£8 11s. 3d.)
Vol. III. Performance, Propulsion, Seaplanes, Stability, Structures, Wind Tunnels. £8 8s. (£8 11s. 6d.)
- 1947 Vol. I. Aerodynamics, Aerofoils, Aircraft. £8 8s. (£8 11s. 9d.)
Vol. II. Airscrews and Rotors, Controls, Flutter, Materials, Miscellaneous, Parachutes, Propulsion, Seaplanes, Stability, Structures, Take-off and Landing. £8 8s. (£8 11s. 9d.)
- 1948 Vol. I. Aerodynamics, Aerofoils, Aircraft, Airscrews, Controls, Flutter and Vibration, Helicopters, Instruments, Propulsion, Seaplane, Stability, Structures, Wind Tunnels. £6 10s. (£6 13s. 3d.)
Vol. II. Aerodynamics, Aerofoils, Aircraft, Airscrews, Controls, Flutter and Vibration, Helicopters, Instruments, Propulsion, Seaplane, Stability, Structures, Wind Tunnels. £5 10s. (£5 13s. 3d.)
- 1949 Vol. I. Aerodynamics, Aerofoils. £5 10s. (£5 13s. 3d.)
Vol. II. Aircraft, Controls, Flutter and Vibration, Helicopters, Instruments, Materials, Seaplanes, Structures, Wind Tunnels. £5 10s. (£5 13s.)
- 1950 Vol. I. Aerodynamics, Aerofoils, Aircraft. £5 12s. 6d. (£5 16s.)
Vol. II. Apparatus, Flutter and Vibration, Meteorology, Panels, Performance, Rotorcraft, Seaplanes. £4 (£4 3s.)
Vol. III. Stability and Control, Structures, Thermodynamics, Visual Aids, Wind Tunnels. £4 (£4 2s. 9d.)
- 1951 Vol. I. Aerodynamics, Aerofoils. £6 10s. (£6 13s. 3d.)
Vol. II. Compressors and Turbines, Flutter, Instruments, Mathematics, Ropes, Rotorcraft, Stability and Control, Structures, Wind Tunnels. £5 10s. (£5 13s. 3d.)
- 1952 Vol. I. Aerodynamics, Aerofoils. £8 8s. (£8 11s. 3d.)
Vol. II. Aircraft, Bodies, Compressors, Controls, Equipment, Flutter and Oscillation, Rotorcraft, Seaplanes, Structures. £5 10s. (£5 13s.)
- 1953 Vol. I. Aerodynamics, Aerofoils and Wings, Aircraft, Compressors and Turbines, Controls. £6 (£6 3s. 3d.)
Vol. II. Flutter and Oscillation, Gusts, Helicopters, Performance, Seaplanes, Stability, Structures, Thermodynamics, Turbulence. £5 5s. (£5 8s. 3d.)
- 1954 Aero and Hydrodynamics, Aerofoils, Arrestor gear, Compressors and Turbines, Flutter, Materials, Performance, Rotorcraft, Stability and Control, Structures. £7 7s. (£7 10s. 6d.)

Special Volumes

- Vol. I. Aero and Hydrodynamics, Aerofoils, Controls, Flutter, Kites, Parachutes, Performance, Propulsion, Stability. £6 6s. (£6 9s.)
Vol. II. Aero and Hydrodynamics, Aerofoils, Airscrews, Controls, Flutter, Materials, Miscellaneous, Parachutes, Propulsion, Stability, Structures. £7 7s. (£7 10s.)
Vol. III. Aero and Hydrodynamics, Aerofoils, Airscrews, Controls, Flutter, Kites, Miscellaneous, Parachutes, Propulsion, Seaplanes, Stability, Structures, Test Equipment. £9 9s. (£9 12s. 9d.)

Reviews of the Aeronautical Research Council

1949-54 5s. (5s. 5d.)

Index to all Reports and Memoranda published in the Annual Technical Reports

1909-1947

R. & M. 2600 (out of print)

Indexes to the Reports and Memoranda of the Aeronautical Research Council

Between Nos. 2451-2549: R. & M. No. 2550 2s. 6d. (2s. 9d.); Between Nos. 2651-2749: R. & M. No. 2750 2s. 6d. (2s. 9d.); Between Nos. 2751-2849: R. & M. No. 2850 2s. 6d. (2s. 9d.); Between Nos. 2851-2949: R. & M. No. 2950 3s. (3s. 3d.); Between Nos. 2951-3049: R. & M. No. 3050 3s. 6d. (3s. 9d.); Between Nos. 3051-3149: R. & M. No. 3150 3s. 6d. (3s. 9d.); Between Nos. 3151-3249: R. & M. No. 3250 3s. 6d. (3s. 9d.); Between Nos. 3251-3349: R. & M. No. 3350 3s. 6d. (3s. 10d.)

Prices in brackets include postage

Government publications can be purchased over the counter or by post from the Government Bookshops in London, Edinburgh, Cardiff, Belfast, Manchester, Birmingham and Bristol, or through any bookseller

© *Crown copyright 1965*

Printed and published by
HER MAJESTY'S STATIONERY OFFICE

To be purchased from
York House, Kingsway, London W.C.2
423 Oxford Street, London W.1
13A Castle Street, Edinburgh 2
109 St. Mary Street, Cardiff
39 King Street, Manchester 2
50 Fairfax Street, Bristol 1
35 Smallbrook, Ringway, Birmingham 5
80 Chichester Street, Belfast 1
or through any bookseller

Printed in England